ISBN: 978-3-95450-247-9 ISSN: 2673-5490 doi: 10.18429/JACoW-IPAC2024-THPS39

CHANNELING PERFORMANCE OF BENT CRYSTALS DEVELOPED AT CERN*

V. Rodin†, O. Aberle, M. Calviani, M. Di Castro, F. Cerutti, Q. Demassieux, L. S. Esposito, S. Gilardoni, A. Lechner, A. P. Marcone, E. Matheson, S. S. Paiva, P. Schoofs, R. Seidenbinder, CERN, Geneva, Switzerland

Abstract

Bent crystals are a mature technology used in several applications at CERN, such as the crystal-assisted collimation system for LHC ion operation and reduction of losses during the slow extraction from the SPS by shadowing the electrostatic septum. In the future, it is planned to measure electric and magnetic dipole moments of short-lived particles with a double-crystal experiment in the LHC. To consolidate their strategic use, CERN has been equipped to produce in-house bent crystals. Each crystal is required to be fully validated before its installation by different techniques, such as metrology, X-ray diffractometry and characterization with beams. The latter can measure the bending angle, the torsion, and the channeling efficiency, which is related to crystal imperfections. In this contribution, we present the performance with beams of the first prototype bent crystals manufactured at CERN and tested during a measurement campaign in the North Area.

INTRODUCTION

The use of planar channeling (CH) in mechanically bent crystals has become an indispensable method for beam manipulations at the CERN accelerator complex. This phenomenon occurs when charged particles entering the crystal with incident angles smaller than $\theta_c = \sqrt{2U_{\max}/p\upsilon}$ with respect to the atomic planes orientation, where $U_{\max}$ is the depth of the inter-planar potential, p and υ are the particle momentum and velocity. A full description of coherent phenomena in crystal lies beyond the scope of this paper, so we refer the reader to previous publications on this topic [1, 2].

Short crystal strips can be cut with respect to specific Miller indices and are mechanically bent to impart an anticlastic curvature [3]. Such crystals can deflect charged particles by tens or hundreds of microradians [4, 5].

Anticlastic crystals are used in several applications at CERN. For example, to improve the collimation efficiency and reduce power load on sensitive equipment in the LHC, crystal-assisted halo collimation [1, 2] has been implemented as a baseline for the $^{208}Pb^{82+}$ beam operation of the HL-LHC upgrade. The system relies on primary beam halo cleaning using bent crystal as primary collimators (TCPCs). The channeled halo particles are absorbed by a secondary collimator and the cleaning efficiency of the collimation system benefits from a reduction of inelastic interactions within the crystal, thus limiting nuclear fragmentation and decreasing collimation losses or activation of sensitive equipment.

Table 1: Main Crystal Target Parameters for LHC and SPS Applications

Ring	Usage	Length, [mm]	Bending angle, [μrad]	Target CH efficiency
LHC	Collim.	4	50.0 ± 2.5	>65%
SPS	Extract.	1	175 ± 75	>55%

Using a similar device in the CERN Super Proton Synchrotron (SPS), the beam losses on a wire-based anode of the electrostatic septum (ZS) are reduced during the resonant slow extraction of 400 GeV/c protons to the North Area. Such scheme is referred to as the "shadowing", since the crystal deflects the protons of the extracted separatrix that would otherwise impinge on the anode wires [5]. At present, about 10^{19}/yr protons are extracted from SPS toward the existing North Area experimental facility. This mitigation will be even more necessary in view of the future flux demand of 4 10^{19} protons on target (POT) per year by the SHiP experiment [6].

The main parameters of crystal assemblies for LHC and SPS applications are reported in Table1 [7, 8].

In order to optimize the deployment of crystal devices in current and upcoming applications [9], a CERN project was initiated to oversee the entire production chain of bent crystal assemblies, from the procurement of low-dislocation crystal wafers to cutting specific crystal strips aligned with the crystal lattice planes, design of bender systems, and their final validation and qualification. The first crystal assembly prototypes were designed and assembled in 2023. They underwent different measurements including metrology, X-ray diffractometry and characterization with 180 GeV/c secondary beam in a test facility at the H8 beam line from the SPS to the North Area [10].

In this paper, we report on the features of first crystal assembly prototypes measured during beam tests in H8 in cooperation with UA9 Collaboration [11]. The particle trajectories were reconstructed with the UA9 tracking detector telescope [12, 13]. Details on analysis methods and evaluation of the crystal defects and impurities are also presented.

DATA ANALYSIS WORKFLOW

In this section, we cover the main aspects of data analysis of crystals measured with beam. Most of the analysis steps closely resemble the procedure proposed by Rossi [14].

* Research supported by the HL-LHC project and CERN SY department.
† volodymyr.rodin@cern.ch

Content from this work may be used under the terms of the CC BY 4.0 licence (© 2024). Any distribution of this work must maintain attribution to the author(s), title of the work, publisher, and DOI.

ISBN: 978-3-95450-247-9 ISSN: 2673-5490 doi: 10.18429/JACoW-IPAC2024-THPS39

© Content from this work may be used under the terms of the CC BY 4.0 licence (© 2024). Any distribution of this work must maintain attribution to the author(s), title of the work, publisher, and DOI.

A crystal is mounted on a goniometer and, in CH orientation, it deflects the incoming particles in the horizontal plane. The experimental setup can measure the impact positions x, y and incoming/outgoing angles θ^{in}, θ^{out} in both horizontal and vertical planes. To accurately assess crystal performance across various track impact positions and angles, it's essential to compensate for macroscopic features in order to homogenize the obtained dataset.

First, a geometrical cut is applied to select tracks with the impact position inside the crystal entry face. The torsion of crystals, t, *i.e.* the twist of the crystal around the vertical axis, is evaluated and numerically compensated to account for the track dependence on the vertical impact parameter. The average offset o of the beam orientation relative to the crystalline plane is measured to take into account the residual angular offset with respect to the crystal optimal channeling orientation. Finally, the mean deflection in amorphous (AM) orientation is evaluated to zero the deflection distribution. The final correcting transformations for the parameters of interest are:

$$\theta_x^{\text{in, corr.}} = \theta_x^{in} + (t.y - o), \quad (1)$$

$$\Delta\theta_x^{\text{corr.}} = \Delta\theta_x - \Delta\theta_{AM}, \quad (2)$$

where t is expressed in µrad/mm and $\Delta\theta_{AM}$ is the average value of the amorphous distribution, *i.e.* beam particles with $|\theta_x^{in}| \gg \Delta\theta_x$.

Some of these steps require tens of fits of the deflection angle ($\Delta\theta_x = \theta_x^{out} - \theta_x^{in}$) distribution that has a Gaussian shape due to the particle scattering with the material budget along the telescope arms and the intrinsic resolution of the trackers. For datasets of crystals with good channeling efficiency (>55%) or large deflection angle, a simple 1D fitting of distribution was found satisfactory. Otherwise, 2D Gaussian fitting of impact distribution in (θ_x^{in}, $\Delta\theta_x$) plane needs to be performed to obtain the mean value of $\Delta\theta_x$.

The single-pass channeling efficiency is defined as the ratio of the particle flux in channeling to the total flux inside the channeling acceptance, i.e. $|\theta_x^{\text{in, corr.}}| < k\,\theta_c$. Two selection criteria are used, particles within one θ_c and, more strictly, within $\theta_c/2$ limit. Further, in the simplest case, we perform a bi-Gaussian fit of the combined AM and CH populations. The efficiency is defined as the ratio of twice the counts of half channeling peak for $\Delta\theta_x^{\text{corr.}} > \Delta\bar{\theta}_x^{CH}$ divided by the size of selection $N(\theta_c, \theta_c/2)$.

Figure 1 depicts most of the described steps, skipping $\Delta\theta_{AM}$ estimate, on a LHC reference crystal data[1].

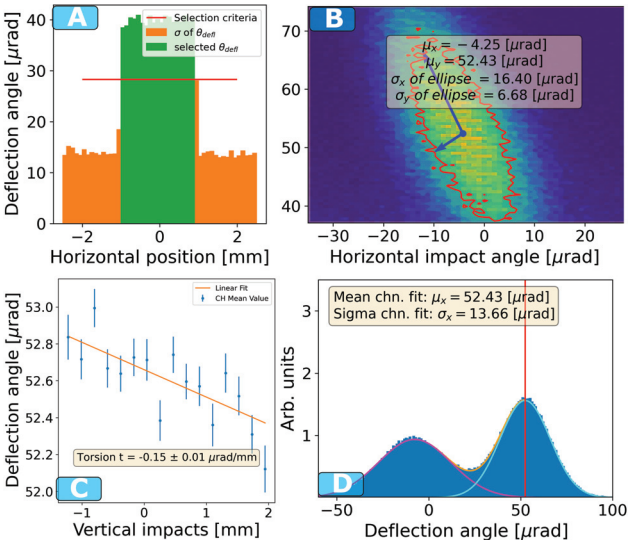

Figure 1: Major steps of the crystal analysis workflow: a) Geometric cuts; b) Offset corrections; c) Torsion evaluation, and d) Final fitting procedure for $\theta_c/2$ selection. The red vertical line in d) indicates the mean deflection angle.

COMPARISON OF ANALYZED CRYSTALS

During the 2023 test campaign, four prototypes underwent thorough examination: three LHC crystals and one SPS. We will refer to them as LHC_CR1-3 and SPS_CR2, respectively. Data for the LHC_CR2 is omitted, as it was not bent. Additionally, some of the analyzed assemblies undergo bake-out, remounting on a translation stage and rebending on the crystal holder. For measurement runs, these manipulations are denoted with suffixes "_TH", "_RM" and "_RB".

The main properties of LHC_CR1,3 and SPS_CR2 are presented in Table 2. From these results, we can see that the channeling efficiency is similar for all crystals. Each crystal's properties are very reproducible by analysis methods if crystal was not rebent. For SPS crystal, however, a smaller statistical population was used due to more tight geometric cuts, resulting in a wider spread in values. All crystals did not meet the required level of channeling efficiency. The deflection of the first LHC crystal fell below the specified threshold, while the deflection of the third LHC crystal met the required criteria. The torsion of the LHC crystals is within the requirement of <1µrad/mm.

Table 2: Main Properties of Examined Prototypes

Crystal	Meas.	CH eff. ($\theta_c/2$) [%]	$\Delta\bar{\theta}_x^{CH}$ [µrad]	t [µrad/mm]
LHC_CR1	7858	50.4±0.40	46.0±0.15	0.4
	7881_RM	50.8±0.27	46.2±0.12	0.3
	7882_RM	50.2±0.21	46.4±0.09	0.2
	7885_RM	50.6±0.20	46.5±0.08	0.3
LHC_CR3	7773	50.8±0.25	49.6±0.11	0.15
	7774	51.0±0.27	49.8±0.10	0.18
	7917_TH	50.3±0.21	49.8±0.10	0.10
	7919_TH	50.3±0.22	49.7±0.10	0.07
SPS_CR2	7783	51.9±0.80	185±0.40	**11.4±1.6**
	7927_TH	52.3±0.89	186±0.40	**12.8±3.3**
	7984_RB	50.5±1.13	192±0.96	**18.0±1.6**
	7985_RB	48.7±1.27	193±0.86	**18.3±2.3**

[1] Crystal from the same batch of the crystals presently installed in the LHC.

ISBN: 978-3-95450-247-9 ISSN: 2673-5490 doi: 10.18429/JACoW-IPAC2024-THPS39

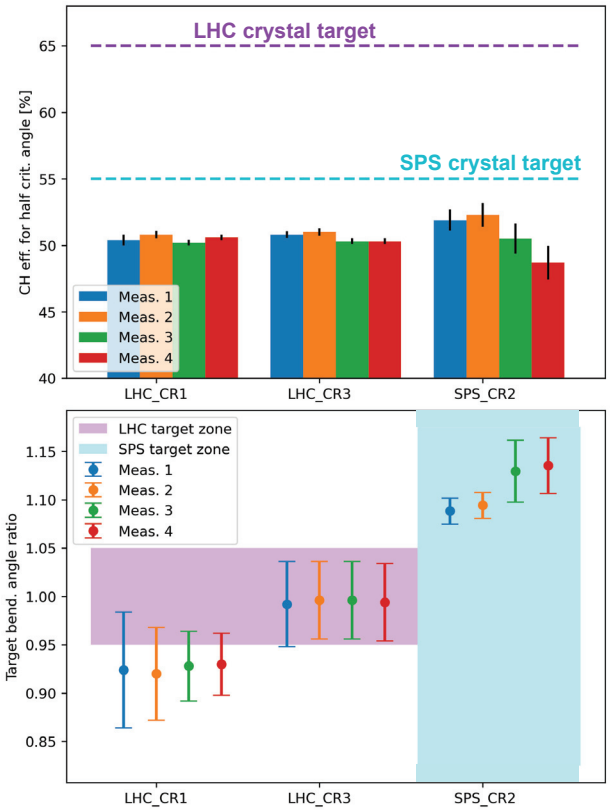

Figure 2: Channeling efficiency (top) and bending angles (bottom) for analyzed LHC and SPS crystals with $|\theta_x^{in}| < \theta_c/2$ selection. Targets are shown for 180 GeV/c protons.

The SPS crystal had the correct bending angle. however due to a larger length (1.1 mm) it developed a large torsion due to extra deformation in its bender as highlighted in the table. A visual summary of these results is shown in Fig. 2.

INDICATION OF ADDITIONAL SILICON DOPING & DEFECTS

All examined crystals, whether bent or unbent, featured decreased channeling efficiency near the edges of the lateral surfaces. An example of this issue is demonstrated in Fig. 3 where a 2D scan was performed to estimate the channeling efficiency of the SPS crystal. For this analysis, the initial geometric cuts in horizontal and vertical planes were meshed to investigate local crystal properties. Each bin had its local corrections following Eq. 1. A significant decrease of the efficiency was observed within 200 µm from the lateral edge. These defects suggest potential shortcomings in the cutting procedures or polishing employed by the manufacturer.

The channeling efficiency of measured crystals was significantly lower than the LHC reference crystal (65 % for $\theta_c/2$). This suggested the presence of crystalline lattice defects or overall impurity of the new crystals. To back up this assumption, the rate of volume reflection (VR) was evaluated for LHC_CR3 and compared with LHC reference crystal, Fig. 4. The volume reflection process unlike channeling

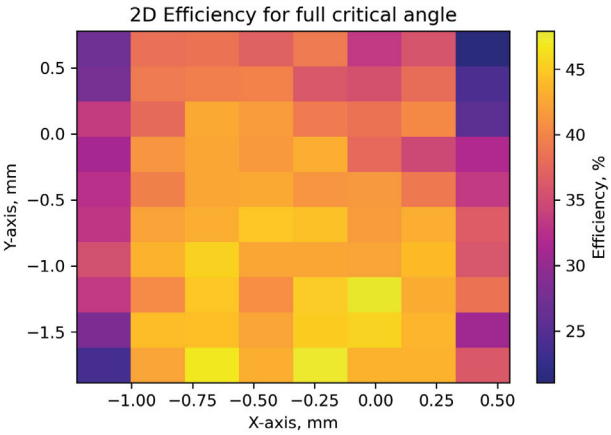

Figure 3: 2D scan of SPS crystal for θ_c selection.

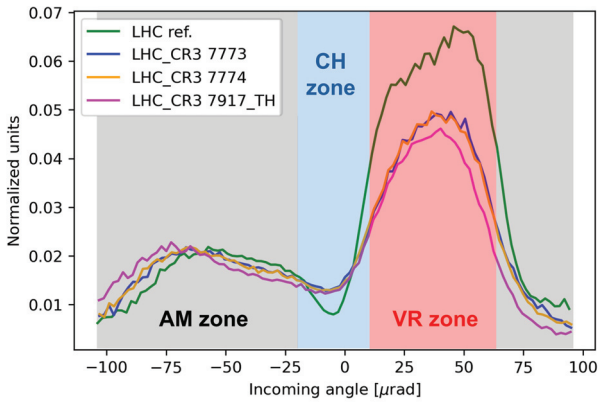

Figure 4: Difference in VR rate for LHC CR3 and reference crystal. Only tracks with $\Delta\theta_x$ between -21.5 and -38.5 µrad were considered in comparison.

is not strongly affected by crystal macroscopic features, so closely linked to the purity of the crystal and the level of defects. The provider later confirmed that the silicon strips were boron-doped, which is consistent with the efficiency reduction.

CONCLUSION & OUTLOOK

After one year of R&D, the first in-house-made prototype of LHC and SPS crystals were successfully assembled and analysed using metrology, X-ray, and beams. The analysis framework provides consistent results across consecutive experimental runs. The reduced efficiency measurement is compatible with doped silicon strips, as confirmed by the provider. The project is on schedule to master the technology. The priorities for 2024 include manufacturing assemblies with undoped crystal, improving the strip machining, and optimizing the lifecycle of the assembly process.

ACKNOWLEDGEMENTS

The authors want to thank the UA9 Collaboration for their important contribution to data taking for access to the data.

Content from this work may be used under the terms of the CC BY 4.0 licence (© 2024). Any distribution of this work must maintain attribution to the author(s), title of the work, publisher, and DOI.

ISBN: 978-3-95450-247-9 ISSN: 2673-5490 doi: 10.18429/JACoW-IPAC2024-THPS39

© Content from this work may be used under the terms of the CC BY 4.0 licence (© 2024). Any distribution of this work must maintain attribution to the author(s), title of the work, publisher, and DOI.

REFERENCES

[1] V. M. Biryukov, Y. A. Chesnokov, and V. I. Kotov, *Crystal Channeling and Its Application at High-Energy Accelerators*. Springer: Berlin, Germany, 1997. doi:10.1007/978-3-662-03407-1

[2] W. Scandale and A. Taratin, "Channeling and volume reflection of high-energy charged particles in short bent crystals. crystal assisted collimation of the accelerator beam halo," *Phys. Rep.*, vol. 815, pp. 1–107, 2019. doi:10.1016/j.physrep.2019.04.003

[3] A. Mazzolari *et al.*, "Silicon crystals for steering high-intensity particle beams at ultrahigh-energy accelerators," *Phys. Rev. Res.*, vol. 3, no. 1, p. 013 108, 2021. doi:10.1103/physrevresearch.3.013108

[4] M. D'Andrea *et al.*, "Crystal Collimation of 20 MJ Heavy-Ion Beams at the HL-LHC," in *Proc. IPAC'21*, Campinas, SP, Brazil, May 2021, pp. 2644–2647. doi:10.18429/JACoW-IPAC2021-WEPAB023

[5] F. M. Velotti *et al.*, "Septum shadowing by means of a bent crystal to reduce slow extraction beam loss," *Phys. Rev. Spec. Top. Accel. Beams*, vol. 22, p. 093 502, 9 2019. doi:10.1103/PhysRevAccelBeams.22.093502

[6] R. Albanese *et al.*, "BDF/SHiP at the ECN3 high-intensity beam facility," CERN, Tech. Rep., 2023. https://cds.cern.ch/record/2878604

[7] R. Bruce, D. Mirarchi, and S. Redaelli, "Functional Specification for Crystal Collimation," CERN, Tech. Rep. LHC-TCPC-ES-0001. https://edms.cern.ch/document/2276602/1.0

[8] M. Fraser, B. Goddard, and F. Velotti, "Requirements of a single thin bent crystal located in LSS4 for the non-local shadowing of the ZS," CERN, Tech. Rep. SPS-TECA-ES-0003. https://edms.cern.ch/document/2377651/1.1

[9] D. Mirarchi, A. S. Fomin, S. Redaelli, and W. Scandale, "Layouts for fixed-target experiments and dipole moment measurements of short-lived baryons using bent crystals at the LHC," *Eur. Phys. J. C*, vol. 80, no. 10, p. 929, 2020. doi:10.1140/epjc/s10052-020-08466-x

[10] G. Brianti, "SPS north experimental area," CERN, Tech. Rep. CERN-SPSC-T-73-8, 1973. https://cds.cern.ch/record/604383

[11] R. Rossi, G. Cavoto, D. Mirarchi, S. Redaelli, and W. Scandale, "Measurements of coherent interactions of 400GeV protons in silicon bent crystals," *Nucl. Instrum. Meth. Phys. Res., Sect. A*, vol. 355, pp. 369–373, 2015. doi:10.1016/j.nimb.2015.03.001

[12] M. Pesaresi *et al.*, "Design and performance of a high rate, high angular resolution beam telescope used for crystal channeling studies," *J. Instrum.*, vol. 6, no. 04, P04006–P04006, 2011. doi:10.1088/1748-0221/6/04/p04006

[13] G. Hall, T. James, and M. Pesaresi, "Optimisation of a silicon microstrip telescope for UA9 crystal channeling studies," *J. Instrum.*, vol. 15, no. 05, p. C05014, 2020. doi:10.1088/1748-0221/15/05/C05014

[14] R. Rossi, L. Esposito, M. Pesaresi, G. Hall, and W. Scandale, "Track reconstruction and analysis of particle interactions in short bent crystals," *J. Instrum.*, vol. 18, no. 06, P06027, 2023. doi:10.1088/1748-0221/18/06/p06027